

Cu₂ZnSnS₄ films fabricated by a simple sol-gel process without sulfurization

ZHANG Ke-Zhi, HE Jun, WANG Wei-Jun, SUN Lin*, YANG Ping-Xiong, CHU Jun-Hao

(Key Laboratory of Polar Materials and Devices, Ministry of Education, East China Normal University, Shanghai 200241, China)

Abstract: Cu₂ZnSnS₄ (CZTS) films with a smooth and compact morphology were obtained via a sol-gel process. Raman spectra and X-ray diffraction (XRD) results indicate that all the films have the kesterite structure. Energy dispersive X-ray spectroscopy (EDS) suggests that all of CZTS films are of S-deficient, Cu-poor and Zn-rich states. The thickness of all the films is around 0.7 μm measured by a field emission scanning electron microscope (FE-SEM). Transmission spectra reveal that the optical band gap (E_g) of samples reduces from 2.13 to 1.52 eV as post-annealing temperature goes up.

Key words: sol-gel, Cu₂ZnSnS₄ (CZTS), film, precursor, pre-anneal, post-anneal, composition

PACS: 68.55.-a, 81.15.Lm, 84.60.Jt

溶胶-凝胶非硫化法制备铜锌锡硫薄膜

张克智, 何俊, 王伟君, 孙琳*, 杨平雄, 褚君浩

(华东师范大学电子工程系极化材料与器件教育部重点实验室, 上海 200241)

摘要: 采用溶胶-凝胶非硫化方法制备了表面平整、致密的铜锌锡硫薄膜。XRD及Raman分析表明制备的铜锌锡硫薄膜为黄铜矿结构。能谱分析表明所有薄膜均贫铜富锌贫硫。场发射扫描电子显微镜测得薄膜的厚度在0.7 μm左右。透射光谱表明随后退火温度的提高薄膜的光学带隙从2.13 eV减小到1.52 eV。

关键词: 溶胶-凝胶; 铜锌锡硫; 薄膜; 前驱体; 预退火; 后退火; 组分

中图分类号: TP914.4 文献标识码: A

Introduction

An increasing amount of attention has been paid to Cu₂ZnSnS₄ (CZTS) thin films^[1-3], as a promising absorber layer material of solar cells. Not only has it good photoelectric properties^[4], but also all elements of CZTS are rich in earth^[3]. CZTS devices have obtained power-conversion efficiency (PCE) up to 8.4%^[5]. Furthermore, the PCE of Cu₂ZnSn(S_xSe_{1-x})₄ (CZTSSe) devices fabricated by Mitzi *et al.* has reached 12.6%^[2]. So, the research of CZTS-base solar cells possess a very good development foreground. However, the theoretical maximum PCE of CZTS devices could be as high as 32%^[6]. Therefore, the PCE of CZTS devices should have more potential in the future.

The preparing methods of CZTS films include physical and chemical techniques^[1,3]. Compared with sputtering^[7-8] and pulsed laser deposition^[9-10], the chemical methods can be used to cut the cost of production^[11]. However, chemical methods to prepare CZTS films generally involve toxic or dangerous raw materials. For example, Mitzi *et al.* fabricated the CZTSSe film by chemical solution-based method and they had to use hydrazine as solvent, which is highly toxic and flammable^[2]. CZTS films fabricated by metal-organics (e. g. Cu(CH₃COO)₂, Zn(CH₃COO)₂) are usual compact and dense^[12-13]. So many researchers, who prepared CZTS films by chemical solution method, prefer to choose metal-organics as raw materials. And they usually select highly toxic 2-methoxyethanol^[12-13] as solvent. To avoid toxic solvent, some researchers have

Received date: 2014-02-10, revised date: 2015-02-02

收稿日期: 2014-02-10, 修回日期: 2015-02-02

Foundation items: Supported by National Natural Science Foundation of China (61106064); Science and Technology Commission of Shanghai Municipality Project (11ZR1411400, 10JC1404600)

Biography: ZHANG Ke-Zhi (1982-), male, Jining, Shandong, PhD candidate. Research involves solar materials and solar cells

* Corresponding author: E-mail: lsun@ee.ecnu.edu.cn

prepared CZTS films by green solvents (e. g. EG^[14], alcohol^[15]) and inorganics (e. g. CuCl₂, ZnCl₂) as raw materials. However, the quality of CZTS films prepared by inorganics raw materials is poorer than those prepared by organics raw materials. Generally there are some cracks or holes in the CZTS films prepared by inorganics^[15]. In this experiment, to obtain the crack-free CZTS films and avoid using toxic solvent, Cu(CH₃COO)₂ · H₂O, Zn(CH₃COO)₂ · 2H₂O, SnCl₂ · 2H₂O and thiourea were chosen as raw materials, and EG was selected as low-toxic solvent.

Generally, H₂S gas was used during the post-annealing process to compensate the loss of S content in CZTS films^[12]. To avoid using toxic H₂S gas, we applied N₂ atmosphere for post-annealing and an excess amount of thiourea was added in the precursor solution, which method was reported to be feasible^[4,15]. Finally, the results of our experiment indicate that the crack-free CZTS films were fabricated via the sol-gel process.

1 Experiment

CZTS precursor solution was fabricated by dissolving Cu(CH₃COO)₂, Zn(CH₃COO)₂, SnCl₂ · 2H₂O and thiourea into EG. The solvent was heated to 100 °C to dissolve the raw materials and prepare CZTS precursor solution. All the materials and solvent were analytical reagents. The initial proportions was Cu: Zn: Sn: S = 2.00: 1.04: 1.20: 8.00^[12,16] and the concentration of cation was around 0.8 M. CZTS precursor films were fabricated by spin-coating CZTS precursor solution onto soda lime glasses (SLG), and then annealed in a rapid thermal processor. To obtain expected thickness, the substrate was coated several times. Every layer of the films was pre-annealed at 300 °C in air, then post-annealed at 400 ~ 500 °C under a N₂ environment to form CZTS phase.

Thermogravimetric analysis (TGA) measurement was performed from 25 to 700 °C in N₂ atmosphere on a thermal-analyzer. The XRD pattern was collected on a diffractometer (Bruker D8 Discover). Raman spectroscopies of samples were collected on a micro-Raman spectrometer (Jobin-Yvon LabRAM HR 800UV) with a 633 nm Ar⁺ laser as the excited light. The spot size and power are 20 μm and 8 mW, respectively. EDX element mapping, component and surface micrograph of samples were observed with a microscope (FE-SEM: Philips XL30FEG). The acceleration voltage applied was 20 kV. Optical transmission spectra was collected on an ultraviolet-visible-near-infrared spectrophotometer (cary500, USA Varian) equipped with integrating sphere.

2 Results and discussions

2.1 Thermal analysis for precursor solution

TGA and DTG (derivative thermogravimetric analysis) results of the CZTS precursor solution are displayed in Fig. 1. As a result of several factors such as dehydration, volatilization and decomposition, there exists weight loss in a broad range. The first step below 170 °C, weight loss ~ 11%, corresponds to dehydration of bound

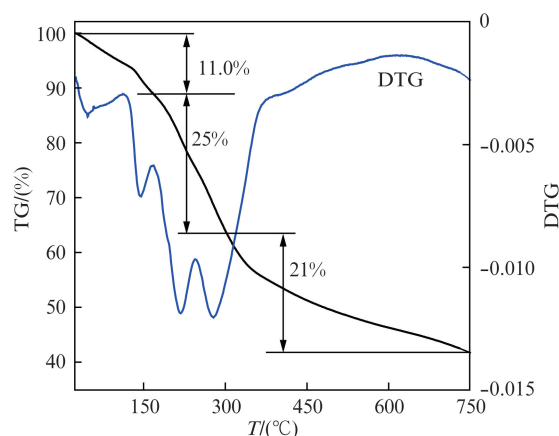


Fig. 1 TGA and DTG of CZTS precursor solution
图1 铜锌锡硫前驱体溶胶的热重及热重微分分析

water in materials and the volatilization of part solvent. The second step between 170 ~ 300 °C, weight loss ~ 25%, is attributed to the decomposition of organics. The third step beyond 300 °C, weight loss ~ 21%, is ascribed to the loss of excess S and volatile metal elements^[17]. Combined with the analysis of TG and DTG, pre-annealing around 300 °C under air atmosphere is necessary to remove organics in the precursor. However, the higher the pre-annealing temperature is, the easier it is for precursor to be oxidized. Thus, the precursors should be pre-annealed at ~ 300 °C exposed to air. To fabricate crystalline CZTS and avoid being oxidized, post-annealing over 300 °C is required under a flowing N₂ atmosphere, which is in good agreement with the previous reports in which CZTS films were synthesized over 300 °C^[4,18].

2.2 Composition analysis of CZTS films

The film pre-annealed only at 300 °C is denoted as S-300, whereas the films pre-annealed at 300 °C and then post-annealed at 400 or 450 or 500 °C are denoted as S-300-400, S-300-450 and S-300-500, respectively. Table 1 shows element ratio of CZTS films deduced from EDX measurements. No other impure elements is detected in the films. C, N and O elements from the slope and raw materials evaporated in gaseous form during pre-annealing or/and post-annealing process. Cl element from the raw material SnCl₂ · 2H₂O may volatilize in the form of HCl. As displayed in table 1, all CZTS films are of S-deficient, Cu-poor and Zn-rich state. The deficiency of Cu and enrichment of Zn is attributed to the initial elemental ratios of CZTS precursor solution, whereas the deficiency of S may be ascribed to the oxidation of thiourea during the pre-annealing period under air atmosphere. Compared with the stoichiometry, the ratio of deficient S increases from 1.4% to 8.8% as post-annealing temperature increases from 300 °C to 500 °C. In Park's study, the CZTS films post-annealed over 500 °C under a N₂ environment had a sulfur content near stoichiometry^[4]. Thus, the preparation process should be optimized to make sulfur content reach the stoichiometry in our future work. In addition, the proportion of Cu in films increases slightly as post-annealing temperature goes up. This observation could be caused by the loss of Zn and Sn metals in post-annealing process.

Table 1 Chemical compositions of CZTS thin films**表 1 CZTS 薄膜的化学组分**

Sample	Cu (at%)	Zn (at%)	Sn (at%)	S (at%)	Cu/(Zn+Sn)	Zn/Sn
S-300	23.5	14.7	12.5	49.3	0.86	1.18
S-300-400	25.2	15.7	12.2	46.9	0.90	1.29
S-300-450	25.8	15.9	12.3	46.0	0.91	1.29
S-300-500	26.0	16.1	12.3	45.6	0.92	1.30

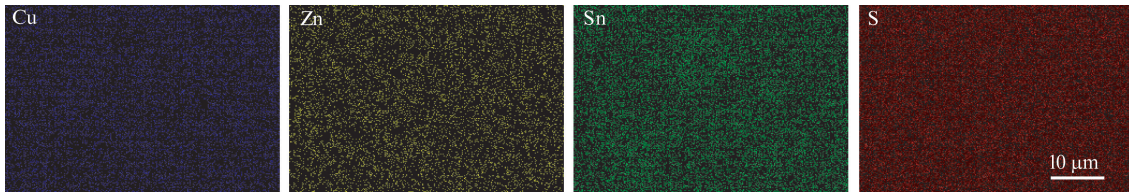


Fig. 2 EDX element mapping for the S-300-500 thin film

图 2 S-300-500 薄膜的组分面扫描

2.3 XRD and Raman spectroscopy analysis

Figure 3 presents the XRD pattern of the CZTS films. As demonstrated in Fig. 3, several diffraction peaks at $\sim 18.2^\circ$, $\sim 28.5^\circ$, $\sim 33.0^\circ$, $\sim 47.5^\circ$ and $\sim 56.3^\circ$ could be attributed to the characteristic peaks for CZTS with a kesterite phase (JCPDS 26-0575). The CZTS films shows one major diffraction peak (112), indicating that they are preferentially oriented in the (112) plane^[10]. When the CZTS precursor is annealed at 300°C , it is partly crystallized, and the solvent and the residual organics are almost removed. The (112) peak becomes sharper as the post-annealing temperature goes up, indicating that high post-annealing temperature is helpful to crystallize, and the preferred orientation of CZTS films becomes obvious. In order to confirm whether there exists second phase in the S-300-500 film, XRD pattern of that sample was also recorded at a low scanning rate. As displayed in Fig. 3(e), some minor peaks appeared which are attributed to the indices of (002), (110), (103), (211) (224) and (008) planes of the CZTS kesterite phase. There are no impure peaks in Fig. 3(e). So, when the post-annealing temperature reaches 500°C , the CZTS films are crystallized well.

For S-300-400 and S-300-450 films, there exist impure peaks near $2\theta = \sim 27.5^\circ$ and $\sim 64.5^\circ$ (marked with “ \blacktriangledown ”, “ \blacklozenge ” symbol in Fig. 3, respectively), which possibly originates from Sn_2O_3 (JCPDS 25-1259) and SnS (JCPDS 34-1439) phase, respectively. It is noted that the crystallization of CZTS could not be determined merely by XRD results. Therefore, Raman spectroscopy is utilized to further identify the phase of CZTS films. Figure 4 displays Raman spectra of CZTS films. The intense peak around 331 cm^{-1} is evidently observed, and it should be ascribed to A_1 mode peak of CZTS films^[3]. A_1 mode peak of CZTS compound is positioned at 338 cm^{-1} in other literatures^[3,19]. There may be exist internal compressive stress in samples, which may be ascribed to the shrinking of substrate when cooling down. The internal stress will cause the A_1 mode peak $\sim 338\text{ cm}^{-1}$ shift slightly to 331 cm^{-1} ^[9]. The peak around 331 cm^{-1} is relatively broad for S-300, and it becomes sharper as the post-annealing temperature goes up. Generally, the intensity and shape of main peaks could show crystalliza-

The homogeneity of CZTS films is an important factor. In order to further prove that the four elements are distributed in the S-300-500 film, EDX element mapping is conducted on the sample. As displayed in Fig. 2, the four elements have been fairly well-distributed on the 2D-projected chemical maps of the S-300-500 film. A homogeneous distribution of the four elements is favorable to the CZTS film used in solar cells.

tion of samples^[20]. This suggests that post-annealing is propitious to the CZTS films crystallize.

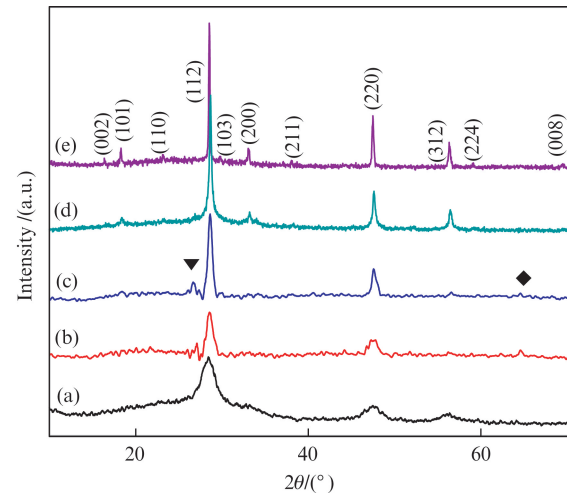


Fig. 3 XRD patterns of CZTS thin films: (a) S-300, (b) S-300-400, (c) S-300-450, (d) S-300-500, (e) XRD at slower scanning velocity for S-300-500

图 3 铜锌锡硫薄膜的 XRD 图: (a) S-300, (b) S-300-400, (c) S-300-450, (d) S-300-500, (e) S-300-500 薄膜的低速扫描 XRD 图

A petty peak around 664 cm^{-1} in all films is a second-order scattering. Two minor peaks at 286 and 368 cm^{-1} are attributed to Raman peaks of CZTS^[10,21]. For the S-300-400 film, the other shoulder peak at 355 cm^{-1} suggests the presence of ZnS ^[10], which usually exists in CZTS films post-annealed under below 450°C . For S-300-400 and S-300-450 films, a minor Raman peak at 465 cm^{-1} corresponds to secondary phase Cu_xS ^[9]. However, the characteristic peaks of Cu_xS are not found in XRD patterns of S-300-400 and S-300-450 films, suggesting the Cu_xS content in them is very little.

From XRD patterns analysis and Raman spectroscopy of samples, we can know that: (1) when post-annealing temperature is at 300°C , only a small amount of CZTS phase is formed, while other sulfides do not appear or are very little; (2) as the post-annealing temperature goes

up, impurity phases such as ZnS, Cu_2S , SnS and Sn_2O_3 are produced; (3) when post-annealing temperature reaches 500 °C, binary sulfides disappear and form CZTS phase, which is agree with the reported literature^[4].

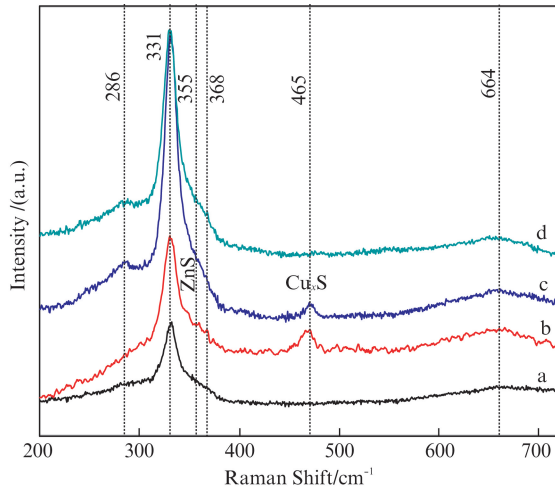


Fig. 4 Raman spectra of CZTS thin films: (a) S-300, (b) S-300-400, (c) S-300-450, (d) S-300-500

图4 铜锌锡硫薄膜的拉曼谱 (a) S-300, (b) S-300-400, (c) S-300-450, (d) S-300-500

2.4 Surface morphology of samples

Figure 5 displays SEM images of CZTS films. The S-300 film has a rough morphology. However, the films that are pre-annealed exposed to air and then post-annealed under a N_2 environment show a good morphology. As demonstrated in Fig. 5 (d) and (e), the S-300-500 film shows a smooth, compact and densely packed morphology without cracks both at the lower- and higher-magnification SEM. The CZTS film with a smooth, compact and crack-free morphology is suitable for absorber layer material in solar cells. While a loose and crack morphology could give rise to stronger recombination losses. The thickness of the S-300-500 sample is about 0.7 μm obtained from Fig. 5 (f), and that of other films is also $\sim 0.7 \mu\text{m}$. Generally, the thickness of CZTS thin films used as absorber layer of solar cells is around 2.0 μm ^[3], and that of our samples could be increased by adding the times of spinning process.

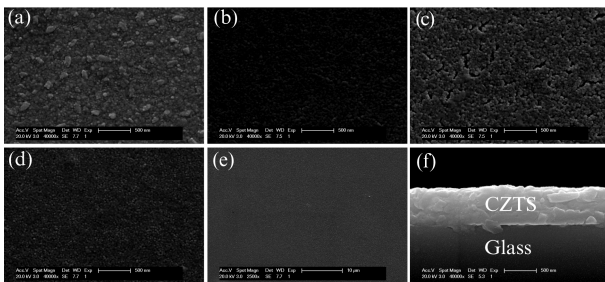


Fig. 5 SEM surface micrographs of CZTS thin films: (a) S-300, (b) S-300-400, (c) S-300-450, (d) S-300-500, (e), (f) the lower-magnification SEM and cross-sectional SEM for S-300-500

图5 铜锌锡硫薄膜的SEM图 (a) S-300, (b) S-300-400, (c) S-300-450, (d) S-300-500, (e)低倍SEM, (f) S-300-500薄膜的截面图

2.5 Optical properties

Transmission spectra and E_g of CZTS films are presented in Fig. 6. The spectra could be simply marked with three characteristic regions: strong absorption, low transmittance and oscillating region (symbolled with “A, B and C”, respectively). The oscillation at wavelength over 1 000 nm derives from interference and reflectance. As displayed in Fig. 6, the absorption edge of films exhibits an obvious red-shift with increasing the post-annealing temperature. Note that there exists a “bad-tail” for the absorption edge of the samples S-300 and S-300-400. This suggests that there could be amorphous or/and impure phase in the films. The value of E_g is obtained from extrapolation of the linear portion of the $(\alpha h\nu)^2$ curve versus the photon energy $h\nu$ to $(\alpha h\nu)^2 = 0$ ^[9]. As demonstrated in the illustration of Fig. 6, these determined E_g of CZTS films (from “a” to “d”) are 2.13, 1.89, 1.65 and 1.52 eV, respectively. The drop in E_g of CZTS films demonstrates that the amount of amorphous and impure phase in the films decrease with the enhancement of the post-annealing temperature. E_g value of the sample S-300-500 is consistent with the reported values in other literature^[12], whereas those of other samples, especially for S-300 and S-300-400, are larger^[12]. It is possibly because that there is ZnS ($E_g = 3.2 \text{ eV}$) in the films which likely occurs at lower post-annealing temperature^[9].

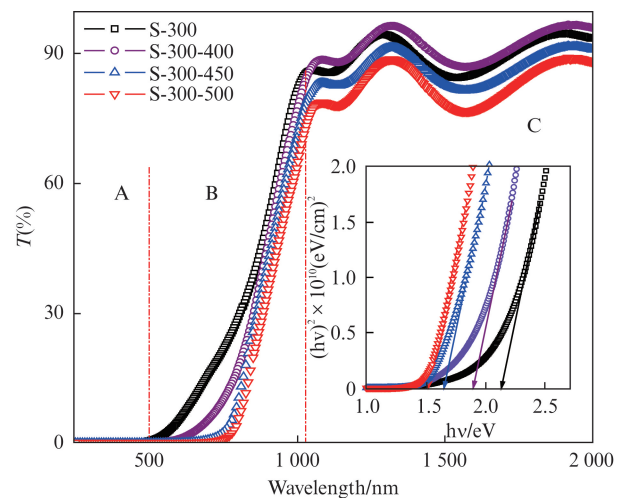


Fig. 6 Transmission spectra and optical band gap of CZTS thin films

图6 铜锌锡硫薄膜的透射光谱及估算光学带隙

3 Conclusions

CZTS films were prepared via a sol-gel process without sulfurization. $\text{Cu}(\text{CH}_3\text{COO})_2 \cdot \text{H}_2\text{O}$, $\text{Zn}(\text{CH}_3\text{COO})_2 \cdot 2\text{H}_2\text{O}$, $\text{SnCl}_2 \cdot 2\text{H}_2\text{O}$ and thiourea were dissolved into low-toxic EG to form CZTS precursor solution; then the so-obtained precursor was spin-coated onto substrates to form precursor films; and finally they were post-annealed under a N_2 atmosphere. All of CZTS films are S-deficient, Cu-poor and Zn-rich state. Following conclusions could be got from XRD patterns of films combined with

Raman spectroscopy: (1) when post-annealing temperature is lower, there is a mixture of CZTS phase and impurity phase such as ZnS, Cu_{2-x}S, SnS and Sn₂O₃; (2) as the post-annealing temperature increases, the binary sulfides react with each other and then form CZTS phase; (3) when post-annealing temperature reaches 500 °C, CZTS kesterite phase is obtained. The film post-annealed at 500 °C under a N₂ environment shows a smooth, compact and crack-free morphology. E_g of CZTS films decreases from 2.13 to 1.52 eV as the post-annealing temperature goes up.

References

- [1] Wang H X. Progress in thin film solar cells based on Cu₂ZnSnS₄[J]. *International Journal of Photoenergy*, 2011; 801292 – 801301.
- [2] Wang W, Winkler M T, Gunawan O, *et al.* Device characteristics of CZTSSe thin-film solar cells with 12.6% efficiency[J]. *Advanced Energy Materials*, 2014, **4**(7): 1301465(1 – 5).
- [3] Mitzi D B, Gunawan O, Todorov T K, *et al.* The path towards a high-performance solution-processed kesterite solar cell[J]. *Solar Energy Materials and Solar Cells*, 2011, **95**: 1421 – 1436.
- [4] Park H, Hwang Y H, Bae B S. Sol-gel processed Cu₂ZnSnS₄ thin films for a photovoltaic absorber layer without sulfurization[J]. *Journal of Sol-Gel Science and Technology*, 2013, **65**: 23 – 27.
- [5] Shin B, Gunawan O, Zhu Y, *et al.* Thin film solar cell with 8.4% power conversion efficiency using an earth-abundant Cu₂ZnSnS₄ absorber [J]. *Progress in Photovoltaics: Research and Applications*, 2013, **21**: 72 – 76.
- [6] Guo Q J, Hillhouse H W, Agrawal R. Synthesis of Cu₂ZnSnS₄ nanocrystal ink and its use for solar cells[J]. *Journal of the American Chemical Society*, 2009, **131**: 11672 – 11673.
- [7] Shin S W, Pawar S M, Park C Y, *et al.* Studies on Cu₂ZnSnS₄ (CZTS) absorber layer using different stacking orders in precursor thin films[J]. *Solar Energy Materials and Solar Cells*, 2011, **95**: 3202 – 3206.
- [8] Seol J S, Lee S Y, Lee J C, *et al.* Electrical and optical properties of Cu₂ZnSnS₄ thin films prepared by rf magnetron sputtering process[J]. *Solar Energy Materials and Solar Cells*, 2003, **75**: 155 – 162.
- [9] Sun L, He J, Kong H, *et al.* Structure, composition and optical properties of Cu₂ZnSnS₄ thin films deposited by pulsed laser deposition method[J]. *Solar Energy Materials and Solar Cells*, 2011, **95**: 2907 – 2913.
- [10] He J, Sun L, Ding N F, *et al.* Single-step preparation and characterization of Cu₂ZnSn(S_xSe_{1-x})₄ thin films deposited by pulsed laser deposition method [J]. *Journal of Alloys and Compounds*, 2012, **529**: 34 – 37.
- [11] Tan H B, Guo C S, Ma X L. Preparation of mullite fibers by Sol-Gel process and study of their morphology[J]. *Materials and Manufacturing Processes*, 2011, **26**: 1374 – 1378.
- [12] Tanaka K, Fukui Y, Moritake N, *et al.* Chemical composition dependence of morphological and optical properties of Cu₂ZnSnS₄ thin films deposited by sol-gel sulfurization and Cu₂ZnSnS₄ thin film solar cell efficiency[J]. *Solar Energy Materials and Solar Cells*, 2011, **95**: 838 – 842.
- [13] Moritake N, Fukui Y, Oonuki M, *et al.* Preparation of Cu₂ZnSnS₄ thin film solar cells under non-vacuum condition [J]. *Physica Status Solidi C*, 2009, **5**: 1233 – 1236.
- [14] Sun Y X, Zong K, Zheng H J, *et al.* Ethylene glycol-based dip coating route for the synthesis of Cu₂ZnSnS₄ thin film [J]. *Materials Letters*. 2013, **92**: 195 – 197.
- [15] Jiang M, Li Y, Dhakal R, *et al.* Cu₂ZnSnS₄ polycrystalline thin films with large densely packed grains prepared by sol-gel method [J]. *Journal of Photonics for Energy*, 2011, **1**: 019501 – 6.
- [16] Guo Q J, Ford G M, Yang W C, *et al.* Fabrication of 7.2% efficient CZTSSe solar cells using CZTS nanocrystals [J]. *Journal of the American Chemical Society*, 2010, **132**: 17384 – 17386.
- [17] Tanaka T, Kawasaki D, Nishio M. Fabrication of Cu₂ZnSnS₄ thin films by co-evaporation [J]. *Physica Status Solidi C*, 2006, **3**: 2844 – 2847.
- [18] Yeh M Y, Lee C C, Wu D S. Influences of synthesizing temperatures on the properties of Cu₂ZnSnS₄ prepared by sol-gel spin-coated deposition [J]. *Journal of Sol-Gel Science and Technology*, 2009, **52**: 65 – 68.
- [19] Fernandes P A, Salome P M P, da Cunha A F. Growth and Raman scattering characterization of Cu₂ZnSnS₄ thin films [J]. *Thin Solid Films*, 2009, **517**: 2519 – 2523.
- [20] Shi J H, Li Z Q, Zhang D W, *et al.* Fabrication of Cu(In,Ga)Se₂ thin films by sputtering from a single quaternary chalcogenide target [J]. *Progress in Photovoltaics: Research and Applications*, 2011, **19**: 160 – 164.
- [21] Zhou S S, Tan R Q, Jiang X, *et al.* Growth of CZTS thin films by sulfurization of sputtered single-layered Cu-Zn-Sn metallic precursors from an alloy target [J]. *Journal of Materials Science: Materials in Electronic*, 2013, **24**: 4958 – 4963.